HHS Public Access

Author manuscript

Oncogene. Author manuscript; available in PMC 2022 April 23.

Published in final edited form as:

Oncogene. 2022 January ; 41(2): 293–300. doi:10.1038/s41388-021-02076-x.

NKX2-1 controls lung cancer progression by inducing DUSP6 to dampen ERK activity

Kelley Ingram[1,2,*], **Shiela C. Samson**[1,2,*], **Rediet Zewdu**[2,3], **Rebecca G. Zitnay**[2,4], **Eric L. Snyder**[1,2,3], **Michelle C. Mendoza**[1,2,4]

[1]Department of Oncological Sciences, University of Utah, Salt Lake City, Utah 84112

[2]Huntsman Cancer Institute, University of Utah, Salt Lake City, Utah 84112

[3]Department of Pathology, University of Utah, Salt Lake City, Utah 84112

[4]Department of Biomedical Engineering, University of Utah, Salt Lake City, Utah 84112

Summary

The RAS→RAF→MEK→ERK pathway is hyperactivated in the majority of human lung adenocarcinoma (LUAD). However, the initial activating mutations induce homeostatic feedback mechanisms that limit ERK activity. How ERK activation reaches the tumor-promoting levels that overcome the feedback and drive malignant progression is unclear. We show here that the lung lineage transcription factor NKX2-1 suppresses ERK activity. In human tissue samples and cell lines, xenografts, and genetic mouse models, NKX2-1 induces the ERK phosphatase DUSP6, which inactivates ERK. In tumor cells from late-stage LUAD with silenced *NKX2-1*, re-introduction of NKX2-1 induces DUSP6 and inhibits tumor growth and metastasis. We show that DUSP6 is necessary for NKX2-1-mediated inhibition of tumor progression *in vivo* and DUSP6 expression is sufficient to inhibit RAS-driven LUAD. Our results indicate that *NKX2-1* silencing, and thereby *DUSP6* downregulation, is a mechanism by which early LUAD can unleash ERK hyperactivation for tumor progression.

Keywords

Lung adenocarcinoma; NKX2-1; DUSP6; ERK

Corresponding author: Michelle.Mendoza@hci.utah.edu.

Contributions

ELS and MCM conceptualized the study. KI, SCS, RGZ, RZ, ELS, and MCM carried out the investigation and extraction of the results. SCS, ELS, and MCM designed the methods and carried out formal analysis and interpretation of the results. MCM managed data curation, project administration, acquisition of study funding, and writing the original manuscript draft. All co-authors were involved in review and editing of the manuscript.

*co-first author

Competing Interests: The authors have no competing financial interests to declare.

Introduction

Lung cancer and specifically lung adenocarcinoma (LUAD) remains the leading cause of cancer death world-wide. The development of therapeutic strategies for long-term patient management requires a better understanding of how cell signaling rewires for tumor progression. The mitogen-activated protein (MAP) kinase extracellular signal-regulated kinase (ERK) is an established initiator and driver of LUAD. ERK is activated downstream of receptor tyrosine kinase signaling to the RAS→RAF→MEK→ERK pathway. More than 60% of LUADs harbor mutations in *RAS* genes, *BRAF*, or *NF1*, which encodes the RAS GTPase activating protein, or upstream receptor tyrosine kinases *EGFR*, *ERBB2*, *MET*, *ALK*, *RET*, and *ROS1* [1, 2]. Mouse models show that these mutations are sufficient to initiate pre-cancerous and low-grade lesions [3–5], but the initial ERK activation is insufficient for progression to metastatic cancer [6, 7].

Active, phosphorylated ERK (p-ERK) is associated with more aggressive LUAD [8, 9] and experiments in mouse models show that increased ERK signaling promotes progression. When *Kras* mutation is combined with *Trp53* or *Lkb1* deletion and given time for the spontaneous acquisition of additional mutations, high-grade metastatic cancer with increased p-ERK develops [3, 6, 10–12]. Furthermore, paradoxical CRAF activation, by inhibition of $BRAF^{V600E}$ in the context of KRAS activation, stimulates ERK activity and accelerates tumor progression [13–15]. How low level ERK activation transitions to high activity sufficient for driving metastasis is unclear.

In addition to exhibiting high ERK activity, the most aggresive LUADs are also poorly differentiated [16, 17]. Mouse models of LUAD suggest that de-differentiation is initiated by loss of the lineage transcription factor NKX2-1/TTF-1 [18–20]. KRAS mutations are inversely correlated with *NKX2-1* expression [21, 22], suggesting RAS-driven LUADs undergo selective pressure to lose NKX2-1. In $KRAS^{G12D}$-driven mouse tumors, *Nkx2-1* deletion increases p-ERK and accelerates progression to invasive carcinoma and metastasis [6, 18, 23]. We reasoned that in addition to beginning the de-differentiation process, *NKX2-1* repression might drive tumor progression by releasing hyperactive ERK.

We sought to identify the mechanism of ERK activation mediated by *NKX2-1* repression. ERK induces negative feedback signaling to upstream components of the RAS pathway, including *Dual-specificity MAPK phosphatases (DUSPs)*. DUSP6 inactivates ERK by dephosphorylating the activation loop [24–26]. DUSP6 is upregulated in early lung cancer lesions with activating *EGFR* or *RAS* mutations [27] and is part of a gene signature that predicts relapse-free and overall survival [28]. *NKX2-1* and *DUSP6* expression positively correlate in human LUAD tumor samples and cell lines [29] and *DUSP6* expression is frequently lost with LUAD progression [30].

We hypothesized that in RAS-driven LUAD, *NKX2-1* silencing removes *DUSP6* expression and elevates ERK activity for tumor growth and metastasis. We found that NKX2-1 loss correlates with reduced DUSP6 in LUAD clinical samples. In LUAD cell lines, NKX2-1 directly induces *DUSP6* expression and limits tumor cell proliferation, migration, invasion, and tumor growth and metastasis. *DUSP6* knockout abrogates the effects of NKX2-1 on

tumor growth. Further, inducing DUSP6 in KRAS-driven tumors shows that the DUSP6-feedback loop is sufficient for NKX2-1 mediated tumor suppression. Our findings indicate that NKX2-1 tempers ERK activity and lung adenocarcinoma progression through the induction of the ERK phosphatase DUSP6.

Results

NKX2-1 transcriptionally induces *DUSP6*.

We tested if NKX2-1 promotes the DUSP6 negative feedback loop that tempers ERK signaling in LUAD. We first compared the amounts of *NKX2-1* and *DUSP6* expression in human LUAD using RNA-seq data from The Cancer Genome Atlas [1]. We also examined *SPROUTY2 (SPRY2)* expression, as SPRY2 inhibits RAF activation and is induced by $KRAS^{G12D}$ mutation in mice [18]. Even though *DUSP6* and *SPRY2* are regulated by multiple transcription factors [31, 32], we found that *DUSP6* and *SPRY2* expression positively correlated with *NKX2-1* mRNA and also with each other (Fig. S1A, B, *NKX2-1* and *DUSP6* r^2=0.28, p=1.8 e^{-12}, *NKX2-1* and *SPRY2* r^2=0.33, p=1.2 e^{-16}, *DUSP6 and SPRY2* r^2=0.49, p=1.4 e^{-36}). We then tested if NKX2-1 protein expression correlates with DUSP6 or SPRY2 in human samples of LUAD using tumor microarrays. NKX2-1 (TTF-1) expression status was provided by the source company, US Biomax, and we performed immunohistochemistry (IHC) for DUSP6 and SPRY2. We found that samples with the highest NKX2-1 intensities (2+ and 3+) contained significantly more DUSP6 than samples lacking NKX2-1 (Fig. 1A, S1C, p=0.001 and 0.002). No association was found between SPRY2 and NKX2-1 (Fig. 1A, S1C). Thus, NKX2-1 correlates with DUSP6 levels, but not SPRY2 levels in human LUAD.

We tested if NKX2-1 is sufficient to induce DUSP6 or SPRY2 in a panel of human LUAD cell lines that contain RAS oncogenes and silenced *NKX2-1*. qRT-PCR showed that exogenous NKX2-1 increased *DUSP6* mRNA (A549 trend with p=0.069, H1299 p=0.003, H23 p=0.020, Fig. 1B). Western blotting showed that NKX2-1 also induced DUSP6 protein (A549 p=0.033, H1299 p=0.007, H23 p=0.002, Fig. 1D). NKX2-1 also increased *SPRY2* mRNA in A549 and H1299 cells (p=0.026 and 0.034), but not in H23 cells (p=0.414, Fig. 1C). SPRY2 protein was universally unaffected (A549 p=0.617, H1299 p=0.098, H23 p=0.493, Fig. 1D). We also tested if NKX2-1 induces *DUSP6* or *SPRY2* in a murine LUAD cell line derived from $KRAS^{G12D}$;$TP53^{Null}$; $NKX2\text{-}1^{Null}$ mouse tumors (3658 cells, [18]). Again, exogenous NKX2-1 increased *Dusp6* mRNA and protein (p=0.003 and 0.022), but not *Spry2* mRNA or protein (p=0.238 and 0.140, Fig. 1E, F).

We tested if NKX2-1 controls *DUSP6* transcription. The promoter region of *DUSP6* is highly conserved in vertebrates and located approximately 1000–250 bp upstream of the transcription start site (*Mm*, [32]). Our previous ChIP-seq of NKX2-1 in $KRAS^{G12D}$ mouse tumors showed NKX2-1 binding within the promoter region of *DUSP6*, with the greatest enrichment between −600 and −400 [18]. Using A549 cells, we assayed the luciferase reporter activity of a promoter construct that included the putative transcription start site at −463 and a portion of the putative NKX2-1 binding region (**191p**, −550 to −359) and a larger construct that included the entire binding region for NKX2-1 (**508p**, −866 to −359). In the absence of NKX2-1, the activity of 191p and 508p was indistinct from the pGL3

vector (Fig. 1G). In the presence of NKX2-1, 508p exhibited 5 times more transcriptional activity than the pGL3 vector (p=0.011, Fig. 1G). However, NKX2-1 alone did not induce the activity of 191p or 508p (V vs NKX2-1 p=0.963 and 0.140, respectively). This suggests that in human lung adenocarcinoma, NKX2-1 induces *DUSP6* mRNA expression to increase DUSP6 protein. However, additional factors recruited to the *DUSP6* promoter may be required to function with NKX2-1 for the induction. The Forkhead box A1/2 (FOXA1/2) proteins are candidate factors, with binding motifs within the *DUSP6* promoter and functional interaction with NKX2-1 in lung cancer metastasis [32–35].

NKX2-1 inhibits cell proliferation, migration, and invasion.

We tested if NKX2-1 inhibits ERK-mediated and DUSP6-regulated cancer phenotypes. NKX2-1 expression uniformly inhibited cell proliferation in A549, H1299, H23, and 3658 cells (Fig. 2A, S2A). Because H1299 cells exhibit the fastest *in vitro* motion of the LUAD lines (Fig. S2B), we used H1299 cells to test if NKX2-1 inhibits migration and invasion. NKX2-1 re-expression slowed 2D migration velocity from 0.33 μm/min to 0.19 μm/min (p=1.8×10^{-9}, Fig. 2B). The reduced migration was similar to treatment with the MEK inhibitor Selumetinib, which reduced movement to 0.22 μm/min (p=7.1×10^{-6}, Fig. 2B). We also tested if NKX2-1 inhibits 3D invasion by embedding H1299 cells as spheroids in collagen I and tracking cell movement. We found that NKX2-1 slowed invasion velocity from 0.257 μm/min to 0.177 μm/min (p=4×10^{-19}, Fig. 2C, S2C). Consistent with previous cell culture studies in which RAS mutation or DUSP6 knockdown caused minimal long-term changes in p-ERK [27, 30, 36], re-introduction of NKX2-1 did not significantly reduce p-ERK upon EGF or PMA stimulation (Fig. S2D, E). Thus, NKX2-1 inhibits cell proliferation, migration, and invasion, but cells in culture adjust their feedback signaling to p-ERK.

NKX2-1 induces DUSP6 and inhibits p-ERK during tumor progression.

We tested if NKX2-1's inhibition of cancer phenotypes is associated with *DUSP6* induction and ERK inhibition *in vivo*, in which more stringent biological pressures for growth and survival model the pathway rewiring of tumorigenesis. Multiple genetically-engineered mouse models of KRAS-driven LUAD have shown that KRAS^{G12D} expression induces NKX2-1-positive tumors (19) and that simultaneous deletion of NKX2-1 with KRAS^{G12D} expression increases tumor cell proliferation and overall tumor burden [18, 37]. We tested if the tumor progression induced by *Nkx2-1* deletion is associated with reduced DUSP6 and increased p-ERK. For this, we used *KRas$^{frtSfrt\text{-}G12D/+}$;Nkx2-1$^{F/F}$;Rosa$^{frtSfrt\text{-}CreERT2}$* mice and intratracheal delivery of FlpO recombinase to activate the *KRas^{G12D}* oncogene and express *Cre^{ERT2}* Cre recombinase. Following 1 week of tumor initiation, mice were treated with Tamoxifen to activate Cre and delete *Nkx2-1*. Twenty weeks after tumor initiation, lungs were harvested and tumors were identified by H&E staining (Fig. S3A). This strategy of removing *Nkx2-1* after tumor initiation results in 60–100% recombination, depending on the mouse, and has a dominant effect with regard to tumor burden when deleted in established tumors ((37), Fig. S3B). NKX2-1 positive and negative tumors were identified by immunohistochemistry (IHC) staining for NKX2-1 and the product of its target gene *pro-surfactant protein B* (*pro-SPB*, Fig. S3B, C). We found that *Nkx2-1* deletion reduced DUSP6 (Fig. S3C) and increased p-ERK and downstream ERK effectors p-RSK and p-S6

(Fig. S3D). *Nkx2-1* deletion also reduced SPRY2 (Fig. S3C), which contrasts with the lack of SPRY2 regulation in the LUAD cell lines.

We tested if NKX2-1 is sufficient for induction of *DUSP6* and inhibition of ERK during tumor growth and metastasis using cell line xenografts. Subcutaneous tumors of A549 cells expressing NKX2-1 were significantly smaller by weight than A549 tumors lacking NKX2-1 (**A549-V** median tumor weight 0.64 g versus **A549-NKX2-1** median 0.17 g, p=0.02, Fig. 2D). 5 out of 9 mice with A549-V tumors exhibited micrometastases to the lung versus 0 out of 9 mice with A549-NKX2-1 tumors (Fig. 2E). IHC showed that tumors lacking NKX2-1 exhibit low DUSP6 expression and high p-ERK, but tumors with NKX2-1 exhibited high DUSP6 expression and reduced p-ERK (Fig. 2F). SPRY2 was not regulated (Fig. 2F).

H1299 cells transplanted orthotopically into mouse lungs showed similar regulation by NKX2-1. The cells were infected for stable expression of GFP-Luciferase and followed by bioluminescence imaging. After 5 weeks of growth, we found that tumors without NKX2-1 grew 9-fold (**H1299-V** normalized median flux 0.7 photon/sec increased to 6.1 photons/sec, p=0.0003, Fig. 2G, H). In contrast, tumors expressing NKX2-1 did not exhibit significant growth (Fig. 2G, H). H1299-NKX2-1 tumors were 3 times smaller than H1299-V tumors (**H1299-NKX2-1** median 1.8 photons/sec, p=0.02, Fig. 2G, H). IHC showed subpopulations with moderate and high NKX2-1 expression (Fig. 2I). Cells with moderate NKX2-1 harbored high DUSP6 expression, but high p-ERK. In contrast, cells with high NKX2-1 harbored moderate increases in DUSP6 and no p-ERK (Fig. 2I, arrows). SPRY2 levels were unchanged. The unexpected population with moderate NKX2-1, but high DUSP6 and p-ERK, is likely a result of re-wiring of the higher basal expression of DUSP6 that we had observed by Western (Fig. 1D). In sum, the A549 and H1299 transplant data are consistent with our hypothesis that NKX2-1-mediated DUSP6 induction limits ERK activation to temper ERK-mediated tumor growth and metastasis.

NKX2-1 drives tumor progression through DUSP6.

We sought to directly test if NKX2-1 acts through DUSP6 to control tumor progression. Previous studies with *DUSP6* knockdown in NHBE and A549 cells did not show regulation of cell growth, suggesting that knockdown efficiency was insufficient to overcome KRAS-induced activation of ERK and expression of DUSP6 [30]. We therefore generated A549 and H1299 *DUSP6* CRISPR/Cas9 knockout clones (Fig. S4A, C). We found that in A549 cells, *DUSP6* knockout (KO) slowed A549 cell proliferation by Day 4 (Fig. S4B), similar to findings that DUSP6 loss can be toxic in LUAD cells that harbor KRAS and EGFR mutations [27]. In H1299 cells, *DUSP6* loss did not change cell proliferation (Fig. S4D), but slowed migration velocity (**control wildtype (WT)** 0.34 μm/min versus ***DUSP6* KO** 0.19 μm/min, $p=7.4\times10^{-16}$, Fig. S4E, F). This suggests that in unpressured cell culture conditions, DUSP6 loss causes toxicity in A549 and H1299 cells.

We aimed to test if NKX2-1 requires DUSP6 to inhibit *in vivo* tumor progression, so introduced TRE-NKX2-1 into the *DUSP6* KO clones of A549 and H1299 cells. Doxycycline induced *NKX2-1* expression in both control WT and *DUSP6* KO cells, and *DUSP6* expression in control cells (Fig. 3A, B). Despite the *in vitro* toxicity of DUSP6 KO noted

above, we characterized the effects of NKX2-1 expression in the absence of DUSP6. We found that in A549 cells, NKX2-1 expression slowed the proliferation of the control WT cells 2.4-fold (Day 6, p=0.01), but not the *DUSP6* KOs (Fig. 3C). Similarly, in H1299 cells, NKX2-1 expression slowed the proliferation of the control WT cells 1.6 fold (Day 6, p=0.03), but not the *DUSP6* KOs (Fig. 3D). NKX2-1 also slowed the migration of control WT cells from 0.32 μm/min to 0.21 μm/min, but did not slow the *DUSP6* KOs (Fig. 3E). While this suggests that NKX2-1 requires DUSP6 to suppress proliferation and migration, the *in vitro* toxicity of DUSP6 KO limits clear conclusions.

We then tested if NKX2-1 acts through DUSP6 to control LUAD progression *in vivo*. We generated subcutaneous tumors with single clones of A549 WT or *DUSP6* KO cells harboring inducible TRE-NKX2-1 and GFP-luciferase. Tumor establishment took 5 weeks for control WT tumors, but 7 weeks for DUSP6 KO tumors because the KO cells initially grew more slowly. However, once tumors were established (150–400 mm^3), both A549 lines grew at the same rate over the ensuing 4 weeks (Fig. 4A, B, +vehicle, median 2.4-fold). We then established tumors in a larger cohort of mice and induced NKX2-1 expression with doxycycline. After 4 weeks of NKX21 induction, control tumors had stopped growing (Fig. 4A, C, +NKX2-1). *DUSP6* KO tumors continued to grow, but at a slower rate than vehicle-treated *DUSP6* KO (median of 1.5-fold). IHC of these final tumors showed that in A549 WT tumors, areas with NKX2-1 expression harbored high DUSP6 expression and low p-ERK (Fig. S5A). A lack of staining for Cleaved Caspase 3 (CC3, Fig. S5A) indicated reduced proliferation, rather than increased apoptosis, is likely the cause of slowed tumor growth following NKX2-1 expression. In contrast, in A549-DUSP6 KO tumors, NKX2-1 expression was not associated with p-ERK and some CC3 staining indicated the presence of apoptosis (Fig. S5A). These results, in which DUSP6 KO toxicity is overcome during *in vivo* growth, indicate that NKX2-1 inhibition of tumor growth requires DUSP6. The results also further support that NKX2-1 regulation of p-ERK requires DUSP6.

We tested if DUSP6 expression is sufficient to temper LUAD tumor growth. We generated tumors in $Kras^{LSL\text{-}G12D/+}$; $Nkx2\text{-}1^{F/F}$ control mice and $Kras^{LSL\text{-}G12D/+}$; $Nkx2\text{-}1^{F/F}$; *CAG-rtTA3* mice [6, 38] using a dual promoter lentivirus that encodes constitutive Cre and doxycycline-inducible *Dusp6* or *Spry2*. The *CAG-rtTA3* transgene drives ubiquitous expression of the tetracycline-regulated transactivator gene. After 5 weeks of tumor growth, a doxycycline diet induced exogenous DUSP6 or SPRY2 in established $KRAS^{G12D}$, $NKX2\text{-}1^{Null}$ tumors. This Cre-mediated strategy of simultaneously initiating tumors and removing NKX2-1 results in a high rate (~96%) of Cre-mediated recombination for *Nkx2-1* deletion (37). H&E staining showed that control mice lacking *rtTA3* harbored multiple large tumors throughout their lungs (Fig. S5B, C, wildtype). The tumors resembled those of our $KRas^{frtSfrt\text{-}G12D/+}$;$Nkx2\text{-}1^{F/F}$;$Rosa^{frtSfrt\text{-}CreERT2}$ mice: low DUSP6 expression and high, uniform p-ERK (Fig. 4D wildtype, Fig. S3C, S3D $NKX2\text{-}1^{Null}$). Mice with the *rtTA3* transgene harbored tumors with heterogeneous HA-tagged DUSP6 and SPRY2 expression, likely due to stochastic silencing of integrated lentivirus following tumor initiation (Fig. 4D, E). Tumors with induced DUSP6 had regressed to small lesions with low p-ERK and DUSP6 expression reduced overall tumor burden (Fig. 4F; Fig. S5B, rtTA3). Consistent with our previous finding that *Nkx2-1* deletion reduces SPRY2 [18] in transgenic mouse tumors, SPRY2 expression reduced tumor size and p-ERK in this system (Fig. 4E, G).

Discussion

Discerning the mechanisms of negative feedback disruption in LUAD *in vivo* is a high priority, as feedback loss is expected to induce tumor progression or alternatively, tumor killing through toxicity. Here, we identify a mechanism of ERK feedback disruption that promotes the progression of *KRAS*-driven mucinous LUAD transitioning through dedifferentiation. NKX2-1 is expressed in alveolar type II cells in the adult, the predominant cell of origin for LUAD [39, 40]. We show that NKX2-1 induces DUSP6. In a genetically-engineered mouse model of LUAD, DUSP6 is downregulated concomitant with NKX2-1. In LUAD cell lines and xenografts, NKX2-1 re-expression causes DUSP6 upregulation. Further, DUSP6 is both necessary and sufficient for NKX2-1 to inhibit *in vivo* ERK activity and tumor growth. We conclude that in early KRAS mutant lesions, NKX2-1's induction of DUSP6 maintains the negative feedback signaling of the RAS→RAF→MEK→ERK pathway and thereby limits ERK activity and tumor progression. NKX2-1 silencing reduces DUSP6, which allows for increased ERK activity that promotes tumor progression during dedifferentiation [19].

Previous analysis of human tumors in the TCGA found that *DUSP6* was the only ERK pathway negative-feedback regulatory gene expressed differently in tumors with *KRAS* or *EGFR* mutations versus tumors lacking ERK pathway mutations [27]. Consistent with this human study, we found that DUSP6, but not SPRY2, correlated with NKX2-1 in human LUAD samples. Further, DUSP6, but not SPRY2, was upregulated upon introduction of NKX2-1 into human LUAD cell lines, both *in vitro* and in xenografts. However, in the genetically engineered mouse tumors, *Nkx2-1* deletion caused a loss of SPRY2 along with a loss of DUSP6. This suggests that NKX2-1 works through DUSP6 in the human disease, but in the $KRAS^{G12D}$ mouse model, NKX2-1 may utilize both DUSP6 and SPRY2 to suppress tumor progression.

Different cell types in the lung have distinct thresholds for oncogenic versus toxic ERK activity, suggesting that NKX2-1-regulated DUSP6 could contribute to a cell type-specific transformation process. Alveolar type II cells transformed by dual *KRas* and *BRaf* mutations suffer toxicity from excessively high p-ERK that occurs with loss of the wildtype *BRaf* allele [14]. In contrast, club cells are transformed by the same high p-ERK and develop into intrabronchiolar lesions [14]. Our data suggest that in KRAS-transformed alveolar type II cells, silencing of NKX2-1 and the resulting reduction in DUSP6 levels increases p-ERK to a sweet spot of tumor-promoting activity without toxic hyperactivity. However, complete knockout of DUSP6 *in vitro* had the opposite effect: cell proliferation and cell migration were slowed. Surprisingly, the same cells showed tumor growth *in vivo*. Our finding indicates that under selective pressure, the tumor cells rewire to adopt an ERK signal intensity that promotes growth and dissemination.

NKX2-1's regulation of DUSP6 to control ERK activation has therapeutic implications. We recently found that $BRAF^{V600E}$; $NKX2\text{-}1^{WT}$ tumor cells exit the cell cycle when treated with BRAF and MEK inhibitors, but NKX2-1-negative persister cells arrest within the cell cycle [37]. Together, the data suggest that the NKX2-1-positive cells are addicted to the lower level of ERK activity maintained in the presence of NKX2-1-induced DUSP6. LUAD

cells with acquired resistance to EGFR inhibitors are similarly addicted to the inhibitor-dampened ERK activity, as inhibitor withdrawal induces toxic ERK hyperactivation [41]. However, decreased *DUSP6* expression and increased ERK activation is an identified resistance mechanism by which LUADs escape therapeutics targeting upstream RAS pathway mutations [42]. Therapeutic strategies to induce tumor-killing by inhibiting DUSP6 and activating ERK are concerning because of *in vivo* tumor heterogeneity and selection. Lineage heterogeneity promotes chemoresistance [20]. Models of tumors with heterogeneous ERK activity show that ERK heterogeneity contributes to differences in transcriptional states that promote tumorigenesis [43]. An NKX2-1-negative subpopulation would contribute to both lineage and ERK activity heterogeneity, both of which would complicate treatment. LUADs harboring NKX2-1 positive and negative cells with different levels of ERK activation will need to be treated differently than tumors with uniform NKX2-1 expression or loss.

Methods

Cell lines and cell culture

A549 ($KRAS^{G12S}$), H1299 ($NRAS^{Q61K}$), H23 ($KRAS^{G12C}$), Phoenix-Ampho, and 293T cells (ATCC) were cultured in DMEM/High Glucose medium (Gibco) with 5% FBS (Sigma).

Tumor xenografts and tumor initiation in genetically engineered mice.—With the University of Utah PRR Core, IACUC #18–11004, subcutaneous tumors were generated and monitored as follows: 5×10^6 A549 cells were mixed with Matrigel and injected subcutaneously into the flank of NSG mice (both male and female mice). Tumor burden of CRISPR KOs was monitored weekly by caliper and bioluminescence measurements (IVIS).

Under University of Utah IACUC #18–08005, $Kras^{LSL\text{-}G12D/+}$; $Nkx2\text{-}1^{F/F}$ mice and $Kras^{LSL\text{-}G12D/+}$; $Nkx2\text{-}1^{F/F}$; *CAG-rtTA3* mice were infected intratracheally with 4×10^4 pfu/mouse lentivirus pCDH-TRE-DUSP6 or pCDH-TRE-SPRY2 that encoded 1) doxycycline inducible *Dusp6* or *Spry2* and 2) constitutive Cre.

Supplementary Material

Refer to Web version on PubMed Central for supplementary material.

Acknowledgements

Thanks to Dr. Stephen Keyse for the gift of the DUSP6 promoter constructs and Dr. Doug Mackay for H2B-mCherry-N2. Thanks to Keith Carney for the development of software for automated cell migration tracking. Flow cytometry was supported by the University of Utah Flow Cytometry Facility and funding from 5P30CA042014-24 and 1S10RR026802-01. Thanks to the University of Utah Cell Imaging Core and the Huntsman Cancer Institute Preclinical Research Resource. M.C.M was supported by K01CA168850, R21CA215891, an American Lung Association Research Grant, American Cancer Society RSG CSM130435, and V Scholar Award. E.L.S. was supported by a Career Award for Medical Scientists from the Burroughs Wellcome Fund, a V Scholar Award, and R01CA212415 and R01CA240317.

References

1. Cancer Genome Atlas Research N. Comprehensive molecular profiling of lung adenocarcinoma. Nature 2014; 511: 543–550. [PubMed: 25079552]
2. Ding L, Getz G, Wheeler DA, Mardis ER, McLellan MD, Cibulskis K et al. Somatic mutations affect key pathways in lung adenocarcinoma. Nature 2008; 455: 1069–1075. [PubMed: 18948947]
3. Dankort D, Filenova E, Collado M, Serrano M, Jones K, McMahon M. A new mouse model to explore the initiation, progression, and therapy of BRAFV600E-induced lung tumors. Genes & development 2007; 21: 379–384. [PubMed: 17299132]
4. Blasco RB, Francoz S, Santamaria D, Canamero M, Dubus P, Charron J et al. c-Raf, but not B-Raf, is essential for development of K-Ras oncogene-driven non-small cell lung carcinoma. Cancer cell 2011; 19: 652–663. [PubMed: 21514245]
5. Trejo CL, Juan J, Vicent S, Sweet-Cordero A, McMahon M. MEK1/2 inhibition elicits regression of autochthonous lung tumors induced by KRASG12D or BRAFV600E. Cancer research 2012; 72: 3048–3059. [PubMed: 22511580]
6. Jackson EL, Olive KP, Tuveson DA, Bronson R, Crowley D, Brown M et al. The differential effects of mutant p53 alleles on advanced murine lung cancer. Cancer research 2005; 65: 10280–10288. [PubMed: 16288016]
7. Johnson L, Mercer K, Greenbaum D, Bronson RT, Crowley D, Tuveson DA et al. Somatic activation of the K-ras oncogene causes early onset lung cancer in mice. Nature 2001; 410: 1111–1116. [PubMed: 11323676]
8. Noguchi M. Stepwise progression of pulmonary adenocarcinoma--clinical and molecular implications. Cancer metastasis reviews 2010; 29: 15–21. [PubMed: 20108111]
9. Vicent S, Lopez-Picazo JM, Toledo G, Lozano MD, Torre W, Garcia-Corchon C et al. ERK1/2 is activated in non-small-cell lung cancer and associated with advanced tumours. Br J Cancer 2004; 90: 1047–1052. [PubMed: 14997206]
10. Feldser DM, Kostova KK, Winslow MM, Taylor SE, Cashman C, Whittaker CA et al. Stage-specific sensitivity to p53 restoration during lung cancer progression. Nature 2010; 468: 572–575. [PubMed: 21107428]
11. Gilbert-Ross M, Konen J, Koo J, Shupe J, Robinson BS, Wiles WGt et al. Targeting adhesion signaling in KRAS, LKB1 mutant lung adenocarcinoma. JCI Insight 2017; 2: e90487. [PubMed: 28289710]
12. Junttila MR, Karnezis AN, Garcia D, Madriles F, Kortlever RM, Rostker F et al. Selective activation of p53-mediated tumour suppression in high-grade tumours. Nature 2010; 468: 567–571. [PubMed: 21107427]
13. Heidorn SJ, Milagre C, Whittaker S, Nourry A, Niculescu-Duvas I, Dhomen N et al. Kinase-dead BRAF and oncogenic RAS cooperate to drive tumor progression through CRAF. Cell 2010; 140: 209–221. [PubMed: 20141835]
14. Nieto P, Ambrogio C, Esteban-Burgos L, Gomez-Lopez G, Blasco MT, Yao Z et al. A Braf kinase-inactive mutant induces lung adenocarcinoma. Nature 2017; 548: 239–243. [PubMed: 28783725]
15. Cicchini M, Buza EL, Sagal KM, Gudiel AA, Durham AC, Feldser DM. Context-Dependent Effects of Amplified MAPK Signaling during Lung Adenocarcinoma Initiation and Progression. Cell reports 2017; 18: 1958–1969. [PubMed: 28228261]
16. Russell PA, Wainer Z, Wright GM, Daniels M, Conron M, Williams RA. Does lung adenocarcinoma subtype predict patient survival?: A clinicopathologic study based on the new International Association for the Study of Lung Cancer/American Thoracic Society/European Respiratory Society international multidisciplinary lung adenocarcinoma classification. J Thorac Oncol 2011; 6: 1496–1504. [PubMed: 21642859]
17. Yoshizawa A, Motoi N, Riely GJ, Sima CS, Gerald WL, Kris MG et al. Impact of proposed IASLC/ATS/ERS classification of lung adenocarcinoma: prognostic subgroups and implications for further revision of staging based on analysis of 514 stage I cases. Mod Pathol 2011; 24: 653–664. [PubMed: 21252858]

18. Snyder EL, Watanabe H, Magendantz M, Hoersch S, Chen TA, Wang DG et al. Nkx2-1 represses a latent gastric differentiation program in lung adenocarcinoma. Molecular cell 2013; 50: 185–199. [PubMed: 23523371]
19. Winslow MM, Dayton TL, Verhaak RG, Kim-Kiselak C, Snyder EL, Feldser DM et al. Suppression of lung adenocarcinoma progression by Nkx2-1. Nature 2011; 473: 101–104. [PubMed: 21471965]
20. Marjanovic ND, Hofree M, Chan JE, Canner D, Wu K, Trakala M et al. Emergence of a High-Plasticity Cell State during Lung Cancer Evolution. Cancer cell 2020; 38: 229–246 e213. [PubMed: 32707077]
21. Takeuchi T, Tomida S, Yatabe Y, Kosaka T, Osada H, Yanagisawa K et al. Expression profile-defined classification of lung adenocarcinoma shows close relationship with underlying major genetic changes and clinicopathologic behaviors. J Clin Oncol 2006; 24: 1679–1688. [PubMed: 16549822]
22. Yatabe Y, Kosaka T, Takahashi T, Mitsudomi T. EGFR mutation is specific for terminal respiratory unit type adenocarcinoma. Am J Surg Pathol 2005; 29: 633–639. [PubMed: 15832087]
23. Maeda Y, Tsuchiya T, Hao H, Tompkins DH, Xu Y, Mucenski ML et al. Kras(G12D) and Nkx2-1 haploinsufficiency induce mucinous adenocarcinoma of the lung. The Journal of clinical investigation 2012; 122: 4388–4400. [PubMed: 23143308]
24. Nunes-Xavier C, Roma-Mateo C, Rios P, Tarrega C, Cejudo-Marin R, Tabernero L et al. Dual-specificity MAP kinase phosphatases as targets of cancer treatment. Anti-cancer agents in medicinal chemistry 2011; 11: 109–132. [PubMed: 21288197]
25. Kidger AM, Keyse SM. The regulation of oncogenic Ras/ERK signalling by dual-specificity mitogen activated protein kinase phosphatases (MKPs). Semin Cell Dev Biol 2016; 50: 125–132. [PubMed: 26791049]
26. Muda M, Theodosiou A, Rodrigues N, Boschert U, Camps M, Gillieron C et al. The dual specificity phosphatases M3/6 and MKP-3 are highly selective for inactivation of distinct mitogen-activated protein kinases. The Journal of biological chemistry 1996; 271: 27205–27208. [PubMed: 8910287]
27. Unni AM, Harbourne B, Oh MH, Wild S, Ferrarone JR, Lockwood WW et al. Hyperactivation of ERK by multiple mechanisms is toxic to RTK-RAS mutation-driven lung adenocarcinoma cells. Elife 2018; 7.
28. Chen HY, Yu SL, Chen CH, Chang GC, Chen CY, Yuan A et al. A five-gene signature and clinical outcome in non-small-cell lung cancer. N Engl J Med 2007; 356: 11–20. [PubMed: 17202451]
29. Watanabe H, Francis JM, Woo MS, Etemad B, Lin W, Fries DF et al. Integrated cistromic and expression analysis of amplified NKX2-1 in lung adenocarcinoma identifies LMO3 as a functional transcriptional target. Genes & development (Research Support, N.I.H., Extramural) 2013; 27: 197–210. [PubMed: 23322301]
30. Okudela K, Yazawa T, Woo T, Sakaeda M, Ishii J, Mitsui H et al. Down-regulation of DUSP6 expression in lung cancer: its mechanism and potential role in carcinogenesis. Am J Pathol 2009; 175: 867–881. [PubMed: 19608870]
31. Ding W, Bellusci S, Shi W, Warburton D. Functional analysis of the human Sprouty2 gene promoter. Gene 2003; 322: 175–185. [PubMed: 14644509]
32. Ekerot M, Stavridis MP, Delavaine L, Mitchell MP, Staples C, Owens DM et al. Negative-feedback regulation of FGF signalling by DUSP6/MKP-3 is driven by ERK1/2 and mediated by Ets factor binding to a conserved site within the DUSP6/MKP-3 gene promoter. Biochem J 2008; 412: 287–298. [PubMed: 18321244]
33. Camolotto SA, Pattabiraman S, Mosbruger TL, Jones A, Belova VK, Orstad G et al. FoxA1 and FoxA2 drive gastric differentiation and suppress squamous identity in NKX2-1-negative lung cancer. Elife 2018; 7.
34. Li CM, Gocheva V, Oudin MJ, Bhutkar A, Wang SY, Date SR et al. Foxa2 and Cdx2 cooperate with Nkx2-1 to inhibit lung adenocarcinoma metastasis. Genes & development 2015; 29: 1850–1862. [PubMed: 26341558]

35. Minoo P, Hu L, Xing Y, Zhu NL, Chen H, Li M et al. Physical and functional interactions between homeodomain NKX2.1 and winged helix/forkhead FOXA1 in lung epithelial cells. Molecular and cellular biology 2007; 27: 2155–2165. [PubMed: 17220277]

36. Gillies TE, Pargett M, Silva JM, Teragawa C, McCormick F, Albeck JG. Oncogenic mutant RAS signaling activity is rescaled by the ERK/MAPK pathway. bioRxiv 2020: 2020.2002.2017.952093.

37. Zewdu R, Mehrabad EM, Ingram K, Jones A, Camolotto SA, Mendoza MC et al. An NKX2-1/ERK/WNT feedback loop modulates gastric identity and response to targeted therapy in lung adenocarcinoma. bioRxiv 2020: 2020.2002.2025.965004.

38. Premsrirut PK, Dow LE, Kim SY, Camiolo M, Malone CD, Miething C et al. A rapid and scalable system for studying gene function in mice using conditional RNA interference. Cell 2011; 145: 145–158. [PubMed: 21458673]

39. Sutherland KD, Song JY, Kwon MC, Proost N, Zevenhoven J, Berns A. Multiple cells-of-origin of mutant K-Ras-induced mouse lung adenocarcinoma. Proceedings of the National Academy of Sciences of the United States of America 2014; 111: 4952–4957. [PubMed: 24586047]

40. Xu X, Rock JR, Lu Y, Futtner C, Schwab B, Guinney J et al. Evidence for type II cells as cells of origin of K-Ras-induced distal lung adenocarcinoma. Proceedings of the National Academy of Sciences of the United States of America 2012; 109: 4910–4915. [PubMed: 22411819]

41. Kong XJ, Kuilman T, Shahrabi A, Oshuizen JB, Kemper K, Song JY et al. Cancer drug addiction is relayed by an ERK2-dependent phenotype switch. Nature 2017; 550: 270–+. [PubMed: 28976960]

42. Hrustanovic G, Olivas V, Pazarentzos E, Tulpule A, Asthana S, Blakely CM et al. RAS-MAPK dependence underlies a rational polytherapy strategy in EML4-ALK-positive lung cancer. Nature medicine 2015; 21: 1038–1047.

43. Davies AE, Pargett M, Siebert S, Gillies TE, Choi Y, Tobin SJ et al. Systems-Level Properties of EGFR-RAS-ERK Signaling Amplify Local Signals to Generate Dynamic Gene Expression Heterogeneity. Cell Syst 2020; 11: 161–175 e165. [PubMed: 32726596]

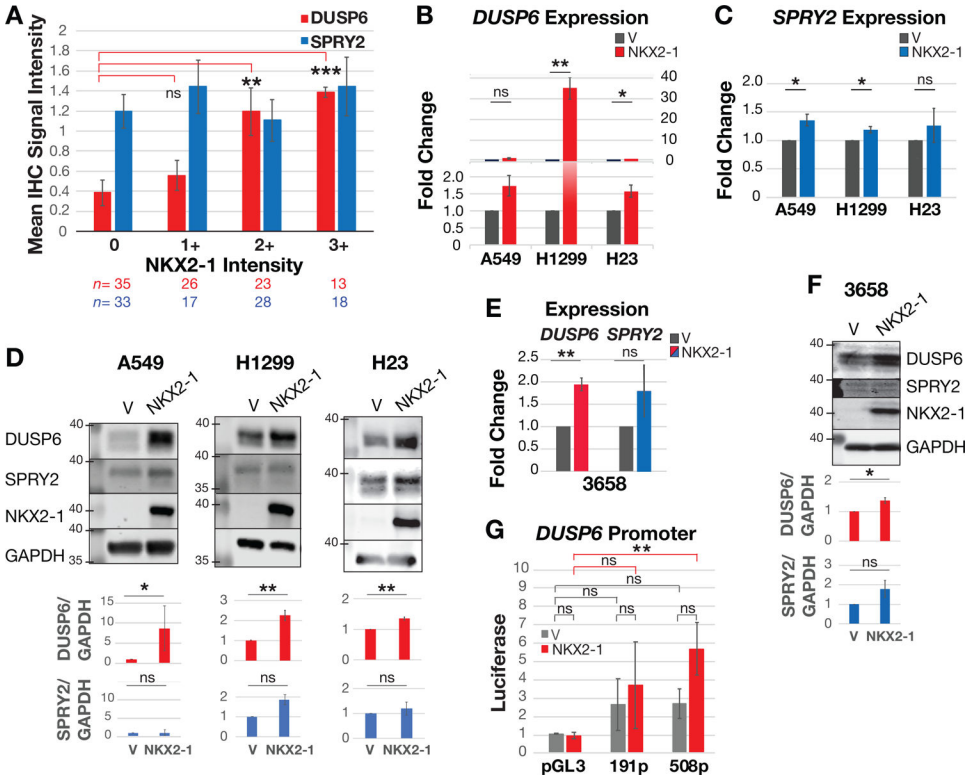

Figure 1. NKX2-1 transcriptionally induces *DUSP6*.

A. IHC intensity scores of DUSP6 and SPRY2 in human LUAD TMAs. Intensities were scored on a scale of 0 (no staining) to 3+ (highest staining). **B**. and **C**. qRT-PCR of *DUSP6* and *SPRY2* upon NKX2-1 expression in cell lines. Mean and SEM for n=3 for A549 and H1299, n=4 for H23. **D**. Westerns of DUSP6 and SPRY2 in LUAD cell lines. V = empty vector. Means and SD. n=4 for A549, n=3 for H1299 and H23. **E**. qRT-PCR of *DUSP6* and *SPRY2* upon NKX2-1 expression in mouse 3658 cells, $KRAS^{G12D}$ n=3. Mean and SEM. **F**. Westerns of DUSP6 and SPRY2 in 3658 cells. Means and SD, n=3. **G**. *DUSP6* luciferase reporter assay, A549 cells. Mean and SEM of normalized luciferase, n=3.

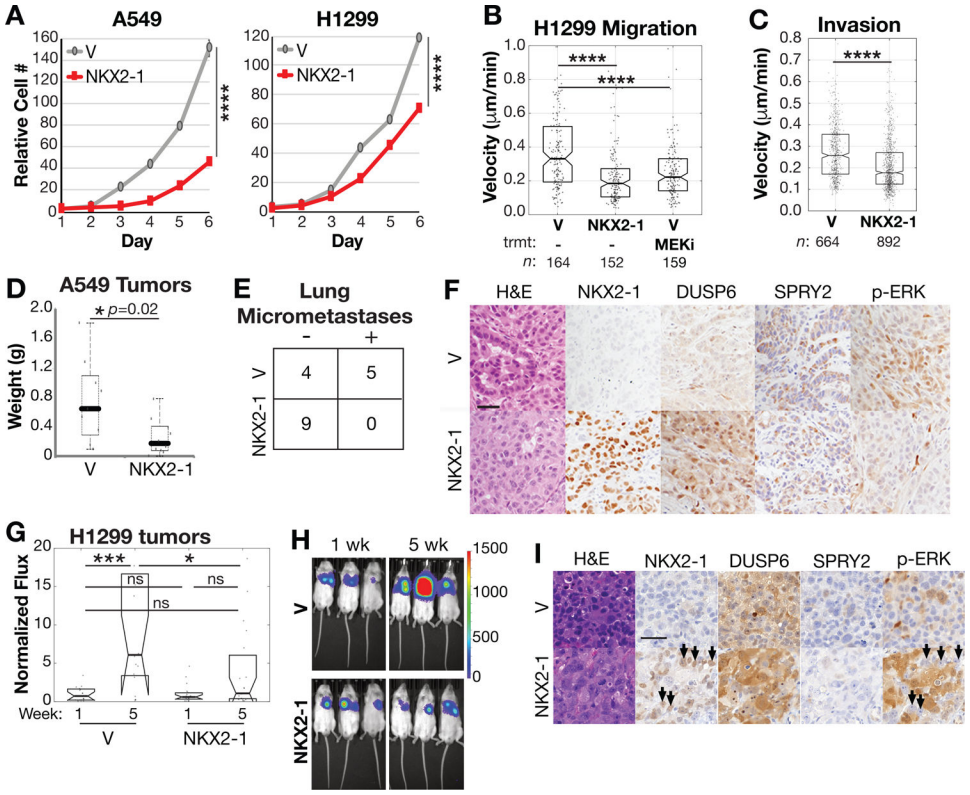

Figure 2. NKX2-1 inhibits cell proliferation, migration and invasion, and tumor growth, dissemination and ERK activity.

A. Cell proliferation. **B**. Migration velocity upon NKX2-1 expression and MEK inhibition (Selumetinib 10 μM). **C**. Invasion velocity as distance/time. **D**. Tumor weight from A549 cells transplanted subcutaneously in mice. p=0.02. Central line is median. Lower and upper box limits are 1st and 3rd quartiles. **E**. Number of mice with lung A549 micrometastases. Fisher's exact test p=0.0294, Chi-square p=0.0085. **F**. H&E and IHC staining in primary A549 tumors. Scale bar 100 μm. **G**. Tumor size in H1299 orthotopic transplants, indicated by total luciferase flux and normalized to initial size at week 1 per cohort. Box center is median. n=16 mice with V, 19 mice NKX2-1. **H**. Representative H1299 IVIS. **I**. IHC of stable H1299 cells transplanted orthotopically into mouse lungs. Images of H&E, NKX2-1, DUSP6, SPRY2, and p-ERK stains. Scale bar 50 μm.

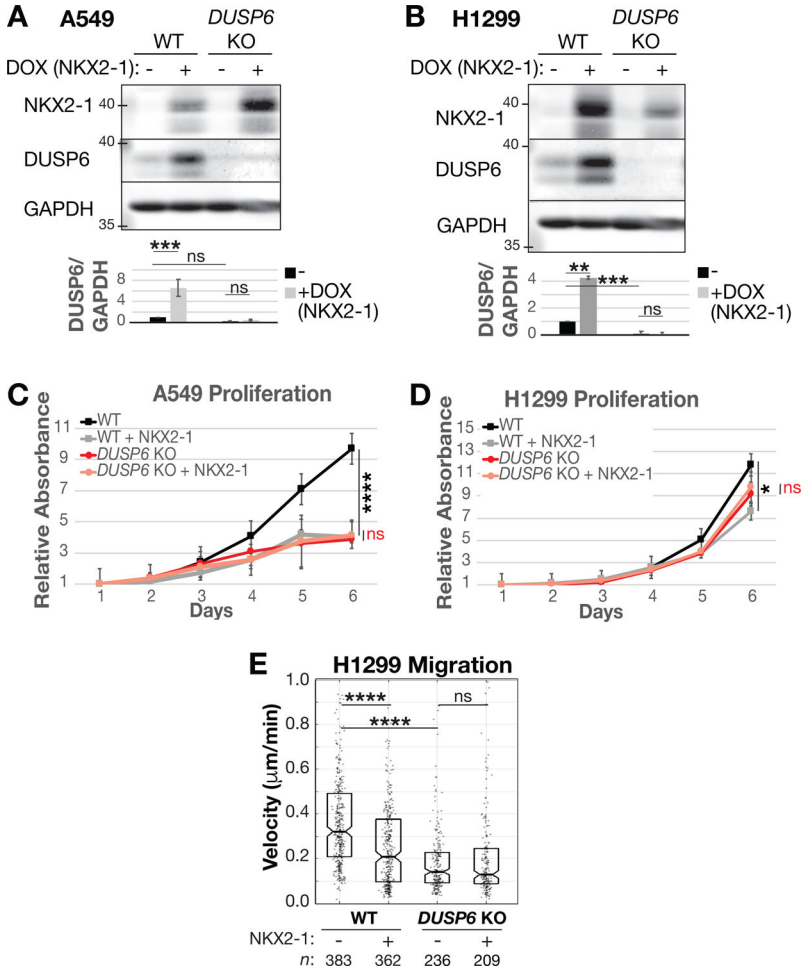

Figure 3. NKX2-1 requires DUSP6 to slow cell proliferation and migration.

A. and **B**. Westerns of A549 and H1299 *DUSP6* knockouts (KOs) with doxycycline (DOX) induction of TRE-NKX2-1. Means and SD, n=3. **C**. and **D**. Cell proliferation upon NKX2-1 induction in A549 and H1299 *DUSP6* KOs. Significance between uninduced and DOX-induced NKX2-1 expression, n=3. **E**. Cell migration upon NKX2-1 induction.

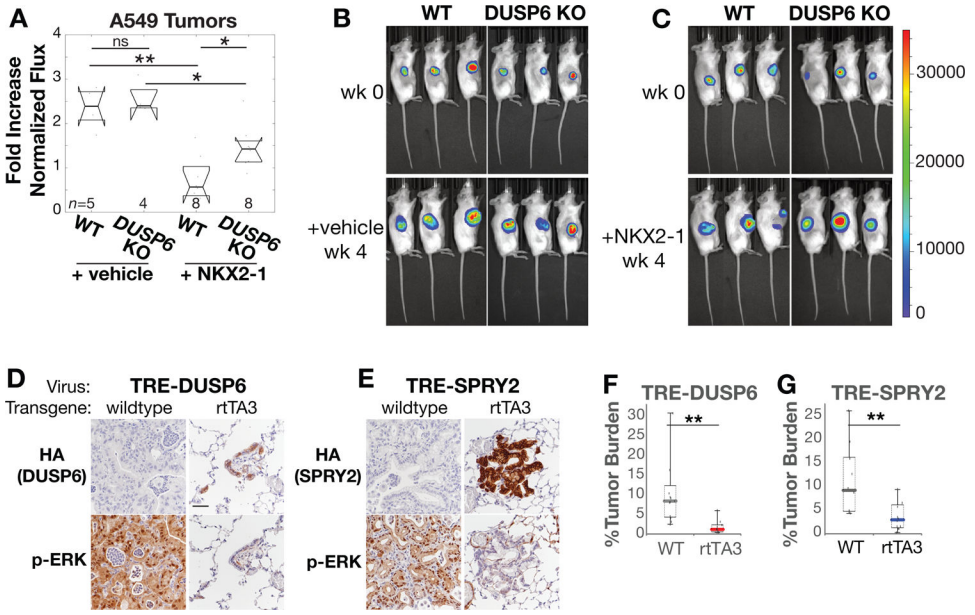

Figure 4. NKX2-1 controls tumor progression through DUSP6.

A. Tumor size in A549 subcutaneous tumors, derived from cell clones in Fig. S4A. Total luciferase flux and normalized to the size at the start of induction of NKX2-1 with DOX. Box center is median. **B**. and **C**. IVIS images for time points in A. **D**. and **E**. IHC for p-ERK in KN-rtTA3 mice infected with TRE-Dusp6 and TRE-Spry2, after 1 week of DOX-mediated de-repression of rtTA3 and induction of DUSP6 or SPRY2. **F**. and **G**. Tumor burden in mice with $KRAS^{G12D}$; $NKX2\text{-}1^{Null}$; WT tumors and $KRAS^{G12D}$; $NKX2\text{-}1^{Null}$; rtTA3 treated with TRE-Dusp6 and TRE-Spry2 for 1 week.